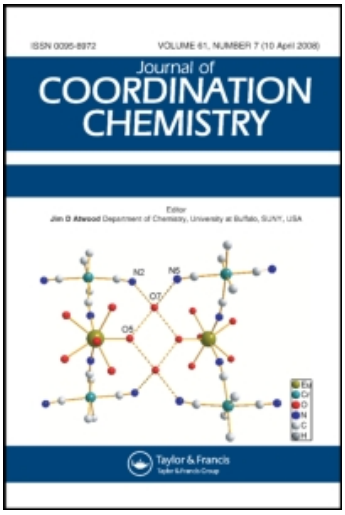

Journal of Coordination Chemistry
Publication details, including instructions for authors and subscription information:
http://www.informaworld.com/smpp/title~content=t713455674

Synthesis and Characterizations of Asymmetrical Dibenzoylmonobenzotetraazacyclo[14]AnnuleneNickel(Ii) Complexes: X-Ray Structure of 3,10-DI(*p*-Chlorobenzoyl)-2,4,9,11-Tetramethyl-1,5,8,12-Monobenzotetraazacyclo[14]AnnuleneNickel(II)

Dong Il Kim[a]; Eun Hee Kim[a]; Sang Hee Shin[a]; Hun Gil Na[b]; Jong Ha Choi[c]; Yu Chul Park[a]
[a] Department of Chemistry, Kyungpook National University, Daegu 702-701, Korea [b] Department of Chemistry, Daejin University, Pochon 487-800, Korea [c] Department of Chemistry, Andong National University, Andong 760-749, Korea

To cite this Article Kim, Dong Il , Kim, Eun Hee , Shin, Sang Hee , Na, Hun Gil , Choi, Jong Ha and Park, Yu Chul(2004) 'Synthesis and Characterizations of Asymmetrical Dibenzoylmonobenzotetraazacyclo[14]AnnuleneNickel(Ii) Complexes: X-Ray Structure of 3,10-DI(*p*-Chlorobenzoyl)-2,4,9,11-Tetramethyl-1,5,8,12-Monobenzotetraazacyclo[14]AnnuleneNickel(II)', Journal of Coordination Chemistry, 57: 2, 133 — 144
To link to this Article: DOI: 10.1080/0095897042000198864
URL: http://dx.doi.org/10.1080/0095897042000198864

J. Coord. Chem., Vol. 57, No. 2, 20 January 2004, pp. 133–144

SYNTHESIS AND CHARACTERIZATIONS OF ASYMMETRICAL DIBENZOYLMONOBENZO-TETRAAZACYCLO[14]ANNULENENICKEL(II) COMPLEXES: X-RAY STRUCTURE OF 3,10-DI(*p*-CHLOROBENZOYL)-2,4,9,11-TETRA-METHYL-1,5,8,12-MONOBENZOTETRAAZA-CYCLO[14]ANNULENENICKEL(II)

DONG IL KIM[a], EUN HEE KIM[a], SANG HEE SHIN[a], HUN GIL NA[b], JONG HA CHOI[c] and YU CHUL PARK[a,*]

[a]*Department of Chemistry, Kyungpook National University, Daegu 702-701, Korea;*
[b]*Department of Chemistry, Daejin University, Pochon 487-800, Korea;*
[c]*Department of Chemistry, Andong National University, Andong 760-749, Korea*

(Received in final form 20 October 2003)

Asymmetric complexes, 3,10-di(*p*-Xbenzoyl)-2,4,9,11-tetramethyl-1,5,8,12-monobenzotetraazacyclo[14]annulenenickel(II), with X=CH_3, H, Cl, NO_2 and OCH_3, have been synthesized and characterized. IR spectra of benzoylated compounds show an intense band attributed to C=O stretching in the region 1627–1655 cm^{-1}. Hammett plots of $1/\lambda_{max}$ of $\pi \rightarrow \pi^*$ and LMCT transitions have positive (+0.224) and negative slopes (−0.250), respectively. ^1H NMR spectra exhibit deshielding effects due to benzoyl groups, while methyl protons show shielding effects. Substituent effects in ^1H and ^{13}C NMR are similar. Voltammograms have two irreversible oxidation peaks due to the ligands in the ranges +290 to +350 mV and +540 to +600 mV, respectively. Reduction and oxidation peaks (metal-based) are found at +0.840 to +0.930 V and −2.580 to −2.840 V, respectively. Hammett plots of the first two oxidation potentials are linear with slopes of +0.028. Metal-based redox potentials (E_{op} and E_{rp}) are dependent on substituents. The structure of the chloro-substituted complex **4** (orthorhombic, $C222_1$, $a = 8.918(5)$, $b = 28.282(5)$, $c = 26.490(5)$ Å, $Z = 4$, $R1 = 0.0392$ and $wR2 = 0.0987$) was solved using single-crystal X-ray diffraction methods.

Keywords: Di(*p*-Xbenzoyl)monobenzotetraazacyclo[14]annulenenickel(II); Spectroscopy; Electrochemistry; X-ray structure

INTRODUCTION

There are many examples of reactions of symmetrical tetraaza[14]annulene metal complexes and the free ligands. For example, reactions of symmetrical tetraaza[14]annulenenickel(II) complexes with electrophiles such as perfluorobenzoyl, azobenzene and benzyl ions have been reported [1–3,9]. The aim of introducing these substituents in

*Corresponding author. Fax: +82-53-950-6330. E-mail: ychpark@knu.ac.kr

ISSN 0095-8972 print: ISSN 1029-0389 online © 2004 Taylor & Francis Ltd
DOI: 10.1080/0095897042000198864

the macrocycle is to prepare new compounds with additional active functional groups [4]. In a previous paper [5], we reported the reaction of 2,4,9,11-tetramethyl-1,5,8,12-*p*-Xbenzotetraazacyclo[14]annulenenickel(II) (X=CH_3, H, Cl, NO_2) with benzoyl chloride.

In this study, we report the synthesis and characterization of asymmetric nickel(II) complexes with monobenzotetraazacyclo[14]annulenes substituted by two *p*-Xbenzoyl groups. We also discuss substituent effects of the X-benzoyl group (X=CH_3, H, Cl, NO_2, OCH_3) on ^1H, ^{13}C NMR, electronic absorption spectra and cyclic voltammetry. The structure of the complex **4** (X=Cl) was determined using X-ray diffraction methods. This study provides information on the reactivity of the methine sites of complex **1** and reaction product.

EXPERIMENTAL

Materials and Measurements

$Ni(OAc)_2 \cdot 4H_2O$, 1,2-phenylenediamine, 1,2-diaminoethane, 2,4-pentandione and Xbenzoyl chloride (X=CH_3, H, Cl, NO_2 and OCH_3) were purchased from Aldrich. The solvents CH_3OH, CH_3CH_2OH and CH_2Cl_2 were refluxed over calcium hydride under nitrogen, and checked for purity by GC before use. Dimethylsulfoxide (DMSO) was purchased from Merck and used without further purification. Tetraethylammonium perchlorate (TEAP), used as supporting electrolyte in electrochemical procedures, was prepared and purified by the method described by Kolthoff and Coetzee [6].

Elemental analyses (C, H, N) of the prepared complex were carried out on a Carlo-Erba EA 1108 instrument. Infrared spectra were recorded on a Matteson Instruments Galaxy 7020A spectrophotometer using KBr Pellets. ^1H and ^{13}C NMR spectra (300 MHz) were recorded on a Bruker instrument at room temperature and chemical shifts in $CDCl_3$ are given in ppm relative to tetramethylsilane as internal reference. Electronic absorption spectra were obtained on a Shimadzu UV-265 spectrophotometer. EI mass spectra were determined with a JEOL MS-DX 300 gas chromatograph mass spectrometer at 70 eV using a direct inlet system.

Cyclic voltammetry was performed using a Bioanalytical System (BAS) CV-50W electrochemical analyzer and C2 cell stand at room temperature. A three-electrode system composed of a glassy carbon working electrode, Ag/Ag^+ (0.01 M $AgNO_3$ in 0.1 M TEAP DMSO solution) as reference electrode and a platinum wire as auxiliary electrode was used for electrochemical measurements.

Synthesis of Complexes

Complex **1**, 2,4,9,11-tetramethyl-1,5,8,12-monobenzotetraazacyclo[14]annulenenickel(II) was prepared by the method reported in the literature [5].

3,10-Di(p-Xbenzoyl)-2,4,9,11-tetramethyl-1,5,8,12-monobenzotetraazacyclo[14]-annulenenickel(II), X=CH_3 (2), H (3), Cl (4), NO_2 (5), OCH_3 (6)

These complexes were prepared by modifying the method reported in the literature [5]. Complex **1** (0.353 g, 0.001 mol) was dissolved in benzene (50 cm^3) containing triethylamine (0.203 g, 0.002 mol) and to this was added the corresponding *p*-Xbenzoyl chloride (0.002 mol) in benzene (30 cm^3) using a dropping funnel. The mixture was

heated under reflux for 4 h with stirring and bubbling nitrogen gas. The reaction mixture was then left standing for 24 h at room temperature and filtered. The filtrate was evaporated to dryness under reduced pressure and the resulting solid recrystallized from a 1 : 2 mixture of dichloromethane and methanol (or *n*-hexane) to give red crystals. For $C_{34}H_{34}N_4O_2Ni$ (**2**): Yield 41%. Anal. Calcd. (%): C, 69.29; H, 5.81; N, 9.51. Found: C, 69.21; H, 5.90; N, 9.50. IR (KBr disc, cm^{-1}): ν(C=C), 1542; ν(C=N), 1603; ν(C=O), 1634; ν(aromatic), 754 and 835. UV-vis: λ_{max} (nm) and ε_{max} ($M^{-1}\,cm^{-1}$) in chloroform 374 and 31 000, and 500 and 7000. EIMS: m/z 588 $[M]^+$. For $C_{32}H_{30}N_4O_2Ni$ (**3**): Yield 43%. Anal. Calcd. (%): C, 68.47; H, 5.39; N, 9.98. Found: C, 68.50; H, 5.39; N, 9.95. IR (KBr disc, cm^{-1}): ν(C=C), 1550; ν(C=N), 1596; ν(C=O), 1655; ν(aromatic), 724 and 805. UV-vis: λ_{max} (nm) and ε_{max} ($M^{-1}\,cm^{-1}$) in chloroform 373 and 33500, and 500 and 7500. EIMS: m/z 560 $[M]^+$. For $C_{32}H_{28}N_4O_2Cl_2Ni$ (**4**): Yield 55%. Anal. Calcd. (%): C, 60.99; H, 4.48; N, 8.89; Found: C, 60.97; H, 4.48; N, 8.88. IR (KBr disc, cm^{-1}): ν(C=C), 1541; ν(C=N), 1583; ν(C=O), 1627; ν(aromatic), 754 and 844. UV-vis: λ_{max} (nm) and ε_{max} ($M^{-1}\,cm^{-1}$) in chloroform 373 and 29 000, and 502 and 7500. EIMS: m/z 629 $[M]^+$. For $C_{32}H_{28}N_6O_6Ni$ (**5**): Yield 35%. Anal. Calcd. (%): C, 59.01; H, 4.33; N, 12.90. Found: C, 59.18; H, 4.21; N, 12.81. IR (KBr disc, cm^{-1}): ν(C=C), 1536; ν(C=N), 1600; ν(C=O), 1633; $\nu(NO_2)$, 1345; ν(aromatic), 741 and 850. UV-vis: λ_{max} (nm) and ε_{max} ($M^{-1}\,cm^{-1}$) in chloroform 368 and 27 500, and 513 and 9500. EIMS: m/z 650 $[M]^+$. For $C_{34}H_{34}N_4O_4Ni$ (**6**): Yield 48%. Anal. Calcd. (%): C, 65.72; H, 5.52; N, 9.02. Found: C, 65.55; H, 5.39; N, 9.02. IR (KBr disc, cm^{-1}): ν(C=C), 1544; ν(C=N), 1595; ν(C=O), 1633; ν(aromatic), 746 and 846. UV-vis: λ_{max} (nm) and ε_{max} ($M^{-1}\,cm^{-1}$) in chloroform 375 and 35 500, and 500 and 7000. EIMS: m/z 620 $[M]^+$.

X-ray Crystallographic Analysis

Preliminary examination and data collection of a crystal of compound **4** was performed with Mo Kα radiation ($\lambda = 0.71069$ Å) on an Enraf–Nonius CAD4 computer-controlled k-axis diffractometer equipped with a graphite-crystal, incident-beam monochromator. Cell constants and orientation matrices for data collection were obtained from least-squares refinement, using the setting angles of 25 reflections. The data were collected for Lorentz-polarization and absorption corrections were applied to the data. The structure was solved by direct methods using SHELXS-86 [7] and refined by full-matrix least-squares calculations with SHELXL-97 [8]. The final cycle of the refinement converged with $R = 0.0392$ and $wR = 0.0987$.

RESULTS AND DISCUSSION

The *p*-Xbenzoylated-tetraazaannulenenickel(II) complexes were prepared by the synthetic procedure of Scheme 1. Reaction of complex **1** with *p*-Xbenzoyl chloride in a 1 : 2 molar ratio was carried out in refluxing benzene in the presence of triethylamine and led to the corresponding products containing two *p*-Xbenzoyl groups (**2**–**6**) with 35–55% yields. Elemental analyses and EI mass spectra of the new complexes are quite consistent with their formulations.

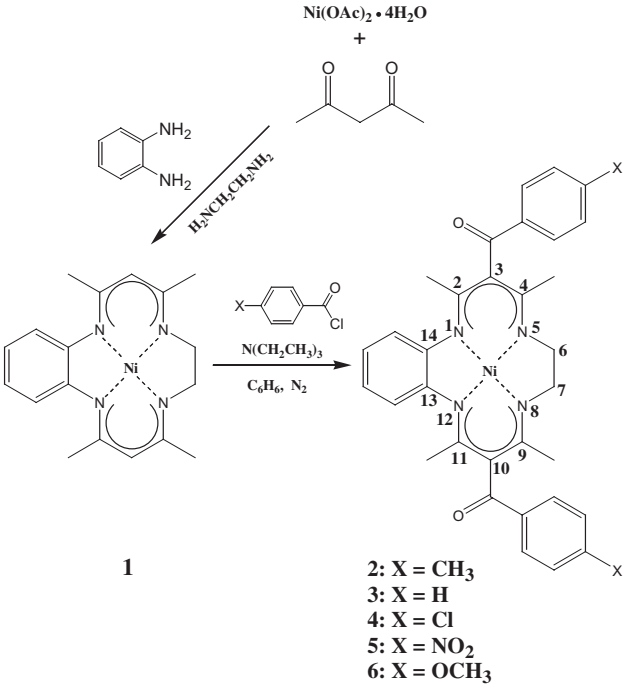

SCHEME 1.

IR and Electronic Absorption Spectra

Characteristic IR absorption data for the complexes are summarized in the Experimental Section. Complexes **2**–**6** exhibited a very intense band in the 1627 to 1655 cm^{-1} region associated with C=O stretching of the benzoyl group. A shift was observed with changing substituents on the benzoyl group, reflecting electronic effects. Complex **5** had a strong band at 1345 cm^{-1} due to the NO_2 group. The benzoyl group has a characteristic mode between 805 and 850 cm^{-1}, while the phenyl group mode of the macrocycle ring appeared between 724 and 754 cm^{-1}. Stretching modes of C=C (1536–1550 cm^{-1}) and C=N (1583–1603 cm^{-1}) groups after benzoylation shifted to higher frequencies by about 20 and 30 cm^{-1}, respectively, compared to complex **1** (1526 and 1564 cm^{-1}).

Electronic absorption spectra of complexes **2**–**6** show two bands in the region 360 to 520 nm. The bands in the near UV region (368–375 nm) with molar absorptivities of 27 000 to 36 000 $M^{-1}\,cm^{-1}$ are attributed to $\pi \rightarrow \pi^*$ transitions. Spectra in the visible region showed bands between 500 and 513 nm ($\varepsilon_{max} = 7000$–$10\,000\ M^{-1}\,cm^{-1}$) attributed to ligand-to-metal charge transfer (LMCT) from the highest occupied ligand molecular orbital to the lowest empty d-orbital of nickel(II). These bands are similar to those of complex **1** but the band at around 500 nm moves to higher energy by about 40 nm, compared with complex **1** (545 nm). Complex **5,** with the *p*-nitrobenzoyl group, has only one charge-transfer band, although it is reported that the complex with NO_2 on a phenyl ring in the macrocycle ring has two charge transfer bands [5c]. The variation of the maximum energies for the electronic transitions of the complexes according to the substituents on the benzoyl group was examined by means of

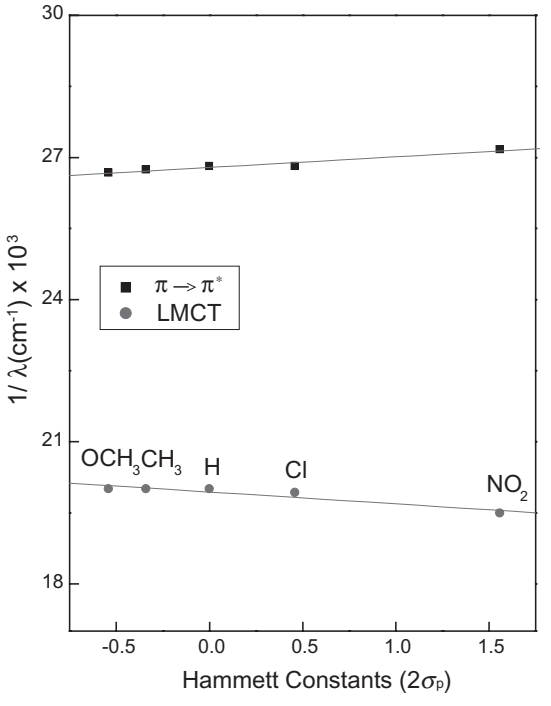

FIGURE 1 Correlations between the maximum energies ($1/\lambda_{max}$) of the $\pi \rightarrow \pi^*$ and LMCT transitions of complexes **2–6** and Hammett constants ($2\sigma_p$).

Hammett plots. As shown in Fig. 1, the energies of $\pi \rightarrow \pi^*$ and the LMCT against substituent constants ($2\sigma_p$: see [10]) of the benzoyl group were linear with a positive slope of $+0.224$ ($\pi \rightarrow \pi^*$) and a negative slope of -0.250 (LMCT), respectively. The slope for $\pi \rightarrow \pi^*$ could be due to expanded π-conjugation. Substituent effects in the phenyl group on the LMCT energies in symmetrical dibenzotetraazacyclo[14]annulene complexes are also negatively correlated ($\rho = -0.72$) [11].

^{1}H and ^{13}C NMR Spectra

The complexes gave well-resolved NMR spectra owing to their diamagnetism. Chemical shift assignments were made on the basis of comparison with complex **1** [5a–c]. Proton NMR data and assignments for the complexes are collected in Table I. The methine proton signals at 3,10-positions of complexes **2–6** disappear upon benzoylation. Methyl proton signals at the 2,4,9,11-positions exhibit upfield shifts of about 0.1 ppm, possibly due to the magnetic anisotropy of the benzoyl group, rather than substituent effects on the phenyl ring of the macrocycle [5c]. Proton resonances at the 6,7-positions of complexes **2–4** and **6** exhibited downfield shifts of around 0.13 ppm relative to those of complex **1**, but those of complex **5** moved upfield by 0.022 ppm owing to the strong electron-withdrawing effect of the nitro group. Similar substituent effects on the phenyl proton signals of the benzoyl group are found. The resonances are affected by both shielding and deshielding effects of the substituents on the benzoyl group.

^{13}C NMR data and assignments are listed in Table II. Carbon peaks of complexes **2–6** are singlets and shifted downfield (except for methyl carbon signals as in the

TABLE I ^{1}H NMR data for monobenzotetraazacyclo[14]annulenenickel(II)

No.	*Methyl*	*Methine*	*Ethylene*	*X*	*Aromatic* (*macrocycle*)	*Aromatic* (*benzoyl*)
1	2.069(s) 2.394(s)	5.042	3.372(s)		6.691–7.185(m)	
2	1.894(s) 2.274(s)		3.510(s)	2.436(s)	6.741–7.059(m)	7.270(d) 7.867(d)
3	1.895(s) 2.295(s)		3.527(s)		6.756–7.062(m)	7.464–7.985(m)
4	1.883(s) 2.286(s)		3.525(s)		6.751–7.072(m)	7.445(d) 7.890(d)
5	1.876(s) 2.328(s)		3.350(s)		6.792–7.082(m)	8.068(d) 8.322(d)
6	1.910(s) 2.277(s)		3.516(s)	3.899(s)	6.731–7.056(m)	6.954(d) 7.953(d)

Chemical shifts in ppm from TMS as internal reference; measured in $CDCl_3$ at 300 MHz; multiplicity of a proton signal is given in parentheses after δ value; s = singlet, d = doublet, t = triplet, m = multiplet.

TABLE II ^{13}C NMR data for monobenzotetraazacyclo[14]annulenenickel(II)

No.	*Methyl*	*Methine*	*Ethylene*	*X*	*Aromatic* (*macrocycle*)	*Aromatic* (*benzoyl*)	*C=N*	*C=O*
1	20.288 23.122	103.856	52.646		119.503 119.997 145.259		154.736 157.886	
2	19.872 21.571	116.121	52.958	22.994	120.538 121.250 138.286	129.323 129.598 143.383 145.211	155.533 158.429	199.281
3	20.066 23.205	116.202	53.055		120.780 121.411 132.591	128.676 129.485 141.053 145.292	156.132 158.834	199.572
4	20.115 23.221	115.814	53.039		120.991 121.444 138.950	128.951 130.795 139.467 145.178	156.277 158.817	198.035
5	20.762 23.755	116.121	53.265		121.703 121.800 146.554	123.948 130.164 145.195 149.935	157.847 159.869	198.806
6	19.742 22.881	115.975	52.974	55.450	120.522 121.266 145.259	113.840 131.847 133.675 163.364	155.161 158.105	198.537

Chemical shifts in ppm from internal TMS; measured in chloroform-*d* at room temperature.

proton NMR). The ethylene carbon signals of the complexes showed regular downfield shifts according to substituents. New carbon signals for carbonyl and phenyl groups after benzoylation were observed at 198–200 ppm and 113–163 ppm, respectively. Trends in the ^{13}C NMR agree with corresponding ^{1}H NMR behaviour.

Electrochemical Behaviour

Redox potentials of the asymmetrical complex **1** and its dibenzoylated compounds measured in 0.1 M TEAP-DMSO solutions *vs* Ag/Ag^+(0.01 M) at 25°C and sweep rates of 100 m V s^{-1} are listed in Table III. Typical voltammograms in the potential range from +1.1 V to −3.0 V *vs* Ag/Ag^+ of the complexes are shown in Fig. 2. Voltammograms of complexes **2**–**6** showed two irreversible oxidation potentials centred on the ligand (Mc) in the ranges +0.290 to +0.600 V ($Mc/Mc^{\bullet+}$ and $Mc^{\bullet+}/Mc^{2+}$) and a metal-based oxidation peak ($Ni^{2+} \rightarrow Ni^{3+}$) between +0.840 and +0.930 V,

TABLE III Redox potential data for monobenzotetraazacyclo[14]annulenenickel(II)

Compound	$E_{op(m)}$, mV $Ni^{2+} \rightarrow Ni^{3+}$	$E_{op(1)}$, mV $0 \rightarrow +1$	$E_{op(2)}$, mV $+1 \rightarrow +2$	$E_{rp(1)}$, mV $0 \rightarrow -1$	$E_{rp(2)}$, mV $-1 \rightarrow -2$	$E_{rp(m)}$, mV $Ni^{2+} \rightarrow Ni^{+}$
1		+98	+567			−2590
2	+860	+300	+550	−2390		−2650
3	+870	+310	+560	−2320		−2640
4	+880	+330	+570	−2090	−2350	−2760
5	+930	+350	+600	−1230	−1760	−2840
6	+840	+290	+540	−2340		−2580

All data were measured in 0.1 M TEAP-DMSO solutions *vs* Ag/Ag^+(0.01 M $AgNO_3$ in DMSO) at 25°C.

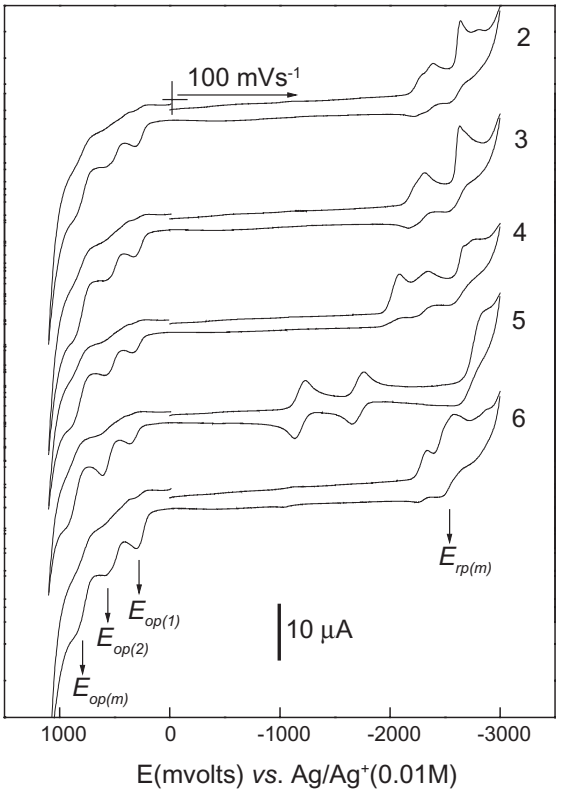

FIGURE 2 Cyclic voltammograms of complexes **2**–**6** (1.0×10^{-3} M) in 0.1 M TEAP–DMSO solutions *vs* Ag/Ag^+ at 25°C.

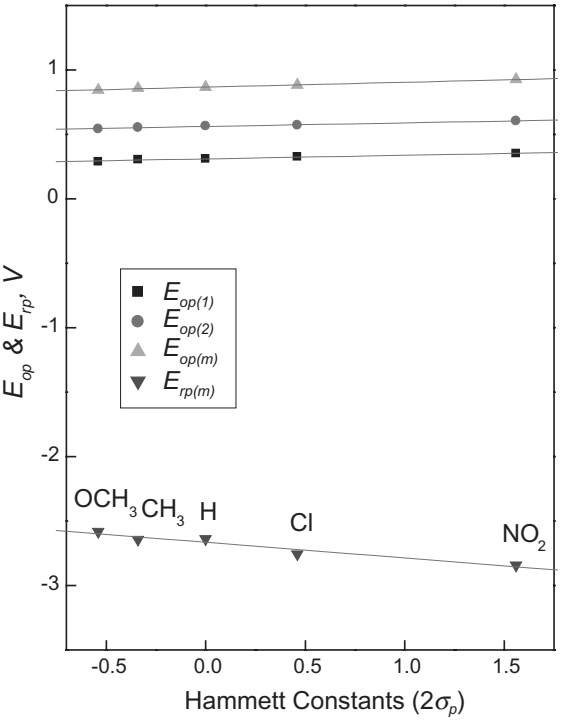

FIGURE 3 Hammett plots of first and second ligand-based oxidation potentials ($E_{op(1)}$ and $E_{op(2)}$), the metal oxidation potential ($Ni^{2+} \rightarrow Ni^{3+}$, $E_{op(m)}$) and the metal reduction potential ($Ni^{2+} \rightarrow Ni^{+}$, $E_{rp(m)}$) against $2\sigma_p$ for complexes **2**–**6**.

respectively. A *quasi* metal reduction peak ($Ni^{2+} \rightarrow Ni^{+}$) showed in the range −2.580 to −2.840 V. The reduction wave of the metal in this solvent are shifted to more positive potentials than in acetonitrile [5c]. Other reduction peaks must be associated with the benzoyl group and their substituents because complex **1** shows only one reduction potential [9]. The oxidation of tetraazaannulene and the reduction of nickel(II) shifted to more positive and negative values according to the electron-withdrawing nature of the substituents on the benzoyl group, respectively. Such redox potentials are scarcely affected by substituents on the benzene group of the macrocyclic ring before benzoylation [12]. Substituent effects were examined by a Hammett plot. As shown in Fig. 3, relationships between redox potentials and $2\sigma_p$ for **2**–**6** were positively (oxidation) or negatively (reduction) linear with slopes of +0.028 for the first and second oxidation potentials ($E_{op(1)}$ and $E_{op(2)}$) that are ligand based, and slopes of +0.038 and −0.122 for the redox potentials ($E_{op(m)}$ and $E_{rp(m)}$) of metal-based reactions, respectively. It is seen that redox potentials are considerably affected by substituents in the benzoyl group in the order: $NO_2 > Cl > H > CH_3 > OCH_3$.

X-ray Structure of Complex 4

The molecular structure of of 3,10-di(*p*-chlorobenzoyl)-2,4,9,11-tetramethyl-1,5,8,12-monobenzotetraazacyclo[14]annulenenickel(II) is illustrated in Fig. 4. Crystal data and refinement parameters are listed in Table IV. The unit cell contains *n*-hexane

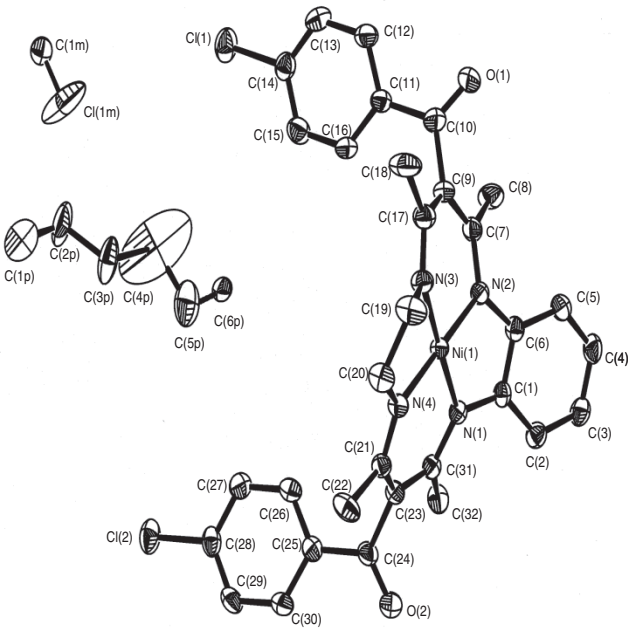

FIGURE 4 X-ray crystal structure of complex **4**, showing the atom numbering scheme.

TABLE IV Crystal data and structure refinement details for complex **4**

Empirical formula	$C_{71}H_{72}Cl_{16}N_8Ni_2O_4$
Formula weight	1431.49
Temperature (K)	173(2)
Wavelength (Å)	0.71069
Crystal system	Orthorhombic
Space group	$C222_1$
Unit cell dimensions (Å)	$a = 8.918(5)$
	$b = 28.282(5)$
	$c = 24.490(4)$
Volume (Å^3)	6681(4)
Z	4
Density (calculated) (Mg m^{-3})	1.423
Absorption coefficient (mm^{-1})	0.859
$F(000)$	2976
Crystal size (mm)	$0.58 \times 0.55 \times 0.10$
θ range for data collection (°)	2.11 to 28.90
Index ranges	$-11 \le h \le 11$
	$-37 \le k \le 30$
	$-17 \le l \le 34$
Reflections collected	17 349
Independent reflections	7986 [R(int) = 0.0276]
Completeness to $\theta = 8.32°$	98.0%
Absorption correction	Semi-empirical from equivalents
Max. and min. transmission	0.9190 and 0.6355
Refinement method	Full-matrix least-squares on F^2
Data/restraints/parameters	7986/9/446
Goodness-of-fit on F^2	1.035
Final R indices [$I > 2\sigma(I)$]	$R1 = 0.0392$, $wR2 = 0.0987$
R indices (all data)	$R1 = 0.0442$, $wR2 = 0.1023$
Absolute structure parameter	0.603(12)
Largest diff. peak and hole (e Å^{-3})	0.829 and −0.557

and dichloromethane solvates, and two molecules of complex **4** as listed in Tables IV and V. Selected bond distances and angles are presented in Table VI. Ni(1)–N(3) [1.849(2) Å] and Ni(1)–N(4) [1.853(2) Å] are somewhat shorter than Ni(1)–N(1) [1.866(2) Å] and Ni(1)–N(2) [1.859(2) Å], while in the symmetrical

TABLE V Atomic coordinates ($\times 10^4$) and equivalent isotropic displacement parameters (Å$^2 \times 10^3$) of non-hydrogen atoms for complex **4**

	x/a	*y/b*	*z/c*	*U(eq)*
Ni(1)	1848(1)	3169(1)	683(1)	21(1)
Cl(1)	8056(1)	4984(1)	2359(l)	46(1)
Cl(2)	8128(1)	1245(1)	2337(l)	44(1)
O(l)	1961(3)	5116(1)	893(1)	54(l)
O(2)	1685(3)	1245(1)	1033(1)	44(l)
N(1)	571(2)	2736(1)	995(1)	23(l)
N(2)	561(2)	3632(1)	930(1)	23(1)
N(3)	3065(3)	3604(1)	361(1)	27(1)
N(4)	3124(3)	2710(1)	428(1)	23(1)
C(1)	−846(3)	2939(1)	1077(1)	24(1)
C(2)	−2216(3)	2698(1)	1130(1)	31(1)
C(3)	−3554(3)	2945(1)	1144(1)	34(1)
C(4)	−3565(3)	3433(1)	1094(1)	37(1)
C(5)	−2230(3)	3679(1)	1032(1)	33(1)
C(6)	−861(3)	3437(1)	1038(1)	26(1)
C(7)	968(3)	4076(1)	1038(1)	28(1)
C(8)	69(4)	4364(1)	1416(1)	39(1)
C(9)	2272(3)	4280(1)	835(1)	29(1)
C(10)	2691(3)	4770(1)	1007(1)	33(1)
C(11)	4045(3)	4822(1)	1334(1)	28(1)
C(12)	4740(4)	5261(1)	1392(1)	35(1)
C(13)	5968(4)	5313(1)	1703(1)	37(1)
C(14)	6500(3)	4924(1)	1962(1)	33(1)
C(15)	5839(4)	4482(1)	1916(1)	36(1)
C(16)	4611(3)	4437(1)	1600(1)	33(1)
C(17)	3186(4)	4056(1)	463(l)	30(1)
C(18)	4304(4)	4357(1)	172(2)	47(1)
C(19)	3779(4)	3392(1)	−84(l)	40(1)
C(20)	4178(3)	2888(1)	47(1)	31(1)
C(21)	3186(3)	2262(1)	563(1)	24(1)
C(22)	4318(4)	1944(1)	306(1)	36(1)
C(23)	2212(3)	2069(1)	938(1)	25(1)
C(24)	2547(3)	1573(1)	1115(1)	29(1)
C(25)	3956(3)	1492(1)	1410(1)	28(1)
C(26)	4647(3)	1864(1)	1660(1)	30(1)
C(27)	5929(3)	1792(1)	1947(1)	34(1)
C(28)	6524(3)	1338(1)	1976(1)	32(1)
C(29)	5870(4)	966(1)	1723(1)	36(1)
C(30)	4578(4)	1043(1)	1444(1)	34(1)
C(31)	954(3)	2293(1)	1136(1)	24(1)
C(32)	76(3)	2041(1)	1549(1)	33(1)
C(1M)	9467(7)	5000	10 000	61(2)
Cl(1M)	8389(3)	4536(1)	9802(1)	198(2)
C(1P)	13 344(13)	3194(5)	2125(2)	53(3)
C(2P)	12 044(9)	3373(5)	2497(7)	135(8)
C(3P)	10 632(8)	3197(5)	2342(4)	56(2)
C(4P)	9073(18)	3378(7)	2619(5)	232(19)
C(5P)	7852(9)	3012(4)	2613(3)	68(3)
C(6P)	6444(9)	3175(4)	3061(4)	47(2)

U(eq) is defined as one third of the trace of the orthogonalized U_{ij} tensor.

TABLE VI Selected bond distances [Å] and angles [°] for complex **4**

Ni(1)–N(1)	1.866(2)	Ni(1)–N(2)	1.859(2)
Ni(1)–N(3)	1.849(2)	Ni(1)–N(4)	1.853(2)
N(2)–C(7)	1.340(3)	N(2)–C(6)	1.413(3)
N(3)–C(17)	1.311(4)	N(3)–C(19)	1.469(4)
N(1)–C(1)	1.405(3)	N(4)–C(20)	1.469(3)
N(1)–C(31)	1.350(3)	N(4)–C(21)	1.318(3)
C(1)–C(6)	1.412(4)	C(7)–C(8)	1.517(4)
C(7)–C(9)	1.404(4)	C(9)–C(17)	1.428(4)
C(9)–C(10)	1.507(4)	C(10)–C(11)	1.494(4)
C(10)–O(1)	1.213(4)	C(14)–Cl(1)	1.749(3)
C(19)–C(20)	1.508(4)	C(17)–C(18)	1.520(4)
C(21)–C(23)	1.428(4)	C(23)–C(31)	1.391(4)
N(1)–Ni(1)–N(2)	85.97(9)	N(4)–Ni(1)–N(1)	94.39(10)
N(4)–Ni(1)–N(3)	86.44(9)	N(4)–Ni(1)–N(2)	179.25(10)
N(3)–Ni(1)–N(1)	178.25(11)	N(3)–Ni(1)–N(2)	93.18(10)
C(6)–N(2)–C(7)	124.4(2)	C(17)–N(3)–C(19)	121.8(2)
C(6)–N(2)–Ni(1)	110.53(17)	C(7)–N(2)–Ni(1)	124.71(19)
C(17)–N(3)–Ni(1)	127.2(2)	C(17)–N(3)–Ni(1)	127.2(2)
N(2)–C(6)–C(1)	113.4(2)	C(19)–N(3)–Ni(1)	110.64(18)
N(2)–C(7)–C(8)	120.1(3)	N(2)–C(7)–C(9)	121.7(2)
N(1)–C(31)–C(23)	121.5(2)	N(1)–C(1)–C(6)	113.9(2)
N(4)–C(21)–C(22)	118.6(2)	N(4)–C(21)–C(23)	122.1(2)
C(21)–C(23)–C(31)	125.3(2)	N(4)–C(20)–C(19)	109.3(2)
C(7)–C(9)–C(10)	117.8(3)	N(3)–C(17)–C(18)	119.7(3)
C(7)–C(9)–C(17)	123.8(2)	N(3)–C(19)–C(20)	107.6(2)
C(9)–C(10)–O(1)	122.3(3)	N(3)–C(17)–C(9)	121.7(3)
C(13)–C(14)–Cl(1)	119.7(2)	C(11)–C(10)–O(1)	119.9(3)

tetraazacyclo[14]-annulenenickel(II) complex the four Ni–N bond distances (1.854 Å) are equal [4]. Bond distances N(3)–C(17) [1.311(3) Å] and N(4)–C(21) [1.318(3) Å] are shorter than N(1)–C(31) [1.350(3) Å] and N(2)–C(7) [1.340(3) Å]. This might be attributable to difference in basicities between phenylenediamine (pK_{a1} and pK_{a2}: 1.81 and 4.61) and ethylenediamine (pK_{a1} and pK_{a2}: 7.08 and 9.89) [13]. The average C–C distance in the six-membered chelate rings is 1.416 Å, similar to those of benzene (1.40 Å), reflecting some aromaticity. On the other hand, C(19)–C(20) [1.508(4) Å] has single-bond character. The average of N–Ni–N angles of five- and six-membered rings are 86.21 and 93.79°, respectively. Angles N(1)–Ni–N(3) and N(2)–Ni–N(4) are 178.25 and 179.25°, respectively, close to square planar, but a little distorted on the basis of the symmetrical tetraazacyclo[14]annulenenickel(II) complex [4]. The benzoyl groups and the four nitrogens are not co-planar. The crystallographic study shows that *n*-hexane and methylene chloride molecules are trapped between molecules of complex **4** and interact only weakly.

Acknowledgement

This work was supported by a Korea Research Foundation Grant (KRF-2002-C00012) to YCP.

Supplementary Data

Full list of Crystallographic data are available from YCP upon request.

References

[1] S.J. Dzugan and D.H. Busch, *Inorg. Chem.* **29**, 2528 (1990).
[2] (a) J. Eilmes, *Polyhedron* **4**, 943 (1985); (b) J. Eilmes, *Polyhedron* **6**, 423 (1987).
[3] (a) K. Sakata, K. Koyanagi and M. Hashimoto, *J. Heterocyclic Chem.* **32**, 329 (1995); (b) K. Sakata, M. Hashimoto, T. Hamada and S. Matsuno, *Polyhedron* **15**, 967 (1996).
[4] E.M. Opozda and W. Lasocha, *Inorg. Chem. Commun.* **3**, 239 (2000).
[5] (a) Y.C. Park, S.S. Kim, D.C. Lee and C.H. An, *Polyhedron* **16**, 253 (1997); (b) Y.C. Park, S.S. Kim, Y.I. Noh and H.G. Na, *J. Coord. Chem.* **41**, 191 (1997); (c) Y.C. Park, H.G. Na, J.H. Choi, J.C. Byun, E.H. Kim and D.I. Kim, *J. Coord. Chem.* **55**, 505 (2002); (d) Y.C. Park, J.C. Byun, J.H. Choi, J.W. Lim, D.C. Lee and H.G. Na, *Polyhedron* **21**, 917 (2002).
[6] I.M. Kolthoff and J.F. Coetzee, *J. Am. Chem. Soc.* **79**, 1852 (1957).
[7] G.M. Sheldrick, *Acta Crystallogr.* **A46**, 467 (1990).
[8] G.M. Sheldrick, SHELX-97 (University of Göttingen, Göttingen, Germany, 1997).
[9] J.C. Dabrowiak, D.P. Fisher, F.C. McElroy and D.J. Macero, *Inorg. Chem.* **18**, 2304 (1979).
[10] N.S. Issaacs, Physical Organic Chemistry (Wiley & Sons, New York, 1995), 2nd Edn., pp. 146–192.
[11] C.L. Bailey, R.D. Bereman, D.P. Rillema and R. Nowak, *Inorg. Chem.* **23**, 3956 (1984).
[12] D.C. Lee, Ph.D. Dissertation (Kyungpook National University, Taegu, Korea, 1998), pp. 702–701.
[13] A. Mederos, S. Domínguez, R.H. Molina and J. Sanchiz and F. Brito, *Coord. Chem. Rev.* **193–195**, 913 (1999).